Journal of Orthopaedic Translation 50 (2025) 413–422

Contents lists available at ScienceDirect

Journal of Orthopaedic Translation

journal homepage: www.journals.elsevier.com/journal-of-orthopaedic-translation

Original Article

Repair of the femoral head osteochondral defect in a swine model using autologous costal cartilage graft transplantation

Fuchou Hsiang [a,1], Yun Gao [a,1], Yiyang Ma [a,1], Peichun Hsu [a], Cheng Qiu [a], Kaiwen Zheng [a], Yidan Pang [a], Jinyu Zhu [a,b], Weibin Yu [a,b], Chun Chen [a], Changqing Zhang [a,2,*], Dajiang Du [a,2,**]

[a] Department of Orthopaedic, Shanghai Jiao Tong University Affiliated Shanghai Sixth People's Hospital, Shanghai, China
[b] Department of Radiology, Shanghai Jiao Tong University Affiliated Shanghai Sixth People's Hospital, Shanghai, China

ARTICLE INFO

Keywords:
Autologous costal cartilage graft
Cartilage repair
Osteochondral defect
Swine model

ABSTRACT

Background: Mosaic transplantation using autologous osteochondral graft (AOCG) is an effective treatment for osteochondral lesion however, at the sacrifice of irreversible damage to the donor articular surface. Costal cartilage is hyaline cartilage and has been utilized as a donor source in various surgeries. This study investigates the use of autologous costal cartilage graft (ACCG) for treating femoral head osteochondral defects in a swine model.

Methods: Osteochondral defects were surgically induced in the femoral heads of one-year-old Bama pigs regardless of sex. The swine were divided into a Defect group without grafting (n = 6), a group grafted with ACCG (n = 6) and a group grafted with AOCG from ipsilateral trochlear groove (n = 6). Postoperatively, swine were allowed free cage activity without immobilization and were euthanized at either 3 or 6 months. Repair effects were evaluated using μCT, MRI, histology and immunohistochemistry (IHC) to assess the osteochondral properties of the grafted femoral head.

Results: There was no difference in the hip function of the Bama pigs between AOCG and ACCG groups. The International Cartilage Repair Society (ICRS) scores showed no difference between AOCG and ACCG at both time points. ACCG exhibited comparable trabecular thickness as AOCG's, but lower trabecular number and higher trabecular separation. Percent bone volume was significantly lower in the ACCG group when compared to AOCG at 3 months, but not at 6 months. Modified MOCART scores were significantly higher in the AOCG group at 3 months but not at 6 months. MRI also detected increasing degree of ossification in the costal cartilage graft at all time points. Histologically, ACCG formed a subchondral bone interface while maintaining the hyaline cartilage characteristics on the articular surface. We also found that superficial layer of ACCG integrated more thoroughly with the recipient cartilage than AOCG did. Furthermore, histology and IHC collectively demonstrated that ACCG had undergone endochondral ossification process at the subchondral layer, evidenced by increased type I collagen expression and decreased type II collagen expression. No donor-site morbidity was noted with ACCG procedure during the study.

Conclusions: This study demonstrates that ACCG can serve as a viable alternative to AOCG for treating femoral head osteochondral defects. The findings show that ACCG offers comparable outcomes to AOCG while avoiding the donor-site morbidity associated with AOCG. Given the challenges related to the donor tissue availability and associated complications in the clinical practice, ACCG could provide a promising and less invasive option for cartilage repair.

* Corresponding author.
** Corresponding author.
E-mail addresses: derek1992725@gmail.com (F. Hsiang), yun_gao@alumni.brown.edu (Y. Gao), mayiyang0709@sjtu.edu.cn (Y. Ma), Eryhsu@outlook.com (P. Hsu), 565525480@qq.com (C. Qiu), zhengkaiwen@sjtu.edu.cn (K. Zheng), pangyidan@hotmail.com (Y. Pang), zjy_1012@126.com (J. Zhu), ywb_abs@163.com (W. Yu), chenchun9@yeah.net (C. Chen), zhangcq@sjtu.edu.cn (C. Zhang), dudajiang@sjtu.edu.cn (D. Du).
[1] The first three authors contributed equally to this manuscript.
[2] The last two authors contributed equally to this manuscript.

https://doi.org/10.1016/j.jot.2024.10.007
Received 3 May 2024; Received in revised form 11 October 2024; Accepted 30 October 2024
Available online 10 February 2025

The translational potential of this article: This proposed method can be translated into practical treatment for repairing osteochondral lesion in human hip joints and provide a new avenue for treating osteochondral lesions in large joints.

1. Introduction

Hip joint arthritis affects up to 10–12 % of the population and the femoral head osteochondral defect is one of the major causes of hip arthritis [1–3]. The repair of osteochondral defects in the deep weight-bearing joints, such as the hip joint, is clinically challenging [4,5]. At present, several surgical treatments such as lesion curettage, marrow stimulation techniques [6], perichondrium grafting, autologous chondrocyte implantation (ACI) and autologous osteochondral graft transplantation (AOCG) are available for small-to moderate-size articular defect [7–11], yet with respective limitations [12].

Marrow stimulating technique such as microfracture induced fibrocartilage filling is related to long-term joint deterioration as the resultant clinical outcomes decrease over time [13]. ACI has been reported as a promising treatment to produce hyaline or hyaline-like cartilage with better durability than fibrocartilage produced by marrow stimulating techniques [14]. However, the limitation of ACI is confined only for the repair of full-thickness cartilage defect in the superficial joints and requires two-stage surgeries [15]. AOCG received promising clinical outcome and has been widely used to treat lesions between 1 and 4 cm^2 [16]. AOCG utilizes hyaline cartilage to repair the defect and can form connection with the recipient articular surface [17–21]. However, AOCG cannot repair widespread lesions due to limited material from of the donor joint [22] and the risk of donor-site morbidity [23]. Thus, it is imperative to find an affluent and safe source of hyaline cartilage for large femoral head osteochondral defect repair.

As hyaline cartilage, costal cartilage is histologically similar to articular cartilage, with affluent source and easy accessibility [24]. The transplantation of the junction of rib and costal cartilage has been applied to the repair and reconstruction of multiple joints [25–27]. In previous small animal experiments, autologous costal cartilage graft (ACCG) transplantation has repaired the knee osteochondral defect through biological integration with the subchondral bone and formed solid osteochondral interface structure with no change of hyaline cartilage morphology [28,29]. Therefore, we attempt to test the feasibility and the reliability of ACCG for femoral head osteochondral defect repair in large animal model by comparing with AOCG (Fig. 1).

2. Materials and methods

2.1. Animals

Eighteen adult Bama pigs (1 year old) were randomly divided into three treatment groups (n = 6 each) [30]. Ventilator support and oxygen inhalation were given during anesthesia. A 6 mm-diameter, 8 mm-deep osteochondral defect was created in the right femoral head. The defect was either left untreated (Defect group) or randomized to grafting with ACCG from right 7th or 8th costal cartilage or AOCG from trochlear groove (Fig. 1). Postoperatively, Bama pigs were allowed for free cage activity without immobilization and were euthanized at 3 or 6 months postoperatively [31]. Weight information of Bama pigs is listed in Supplementary Table 1. All procedures in the present study were strictly executed in accordance with the ethic committee of Shanghai 6th People's Hospital (Animal Welfare Ethics Acceptance #: DWLL2021-0852; Animal Experiment Registry #: DWSY2018-0195).

2.2. Model creation and postoperative care

AOCG collection: To access the trochlear groove, an 8 cm long skin incision was made at the medial aspect of the patella. Following the medial knee arthrotomy, the patella was subluxated to the lateral side to expose the trochlear groove. AOCG was collected using a 6 mm-diameter biopsy punch of 8 mm in depth.

ACCG collection: After the osseocartilaginous junction was exposed via lateral subaxillary approach, ACCG was harvested directly from the right 7th or 8th cartilaginous part of rib without bony part using a 6 mm-

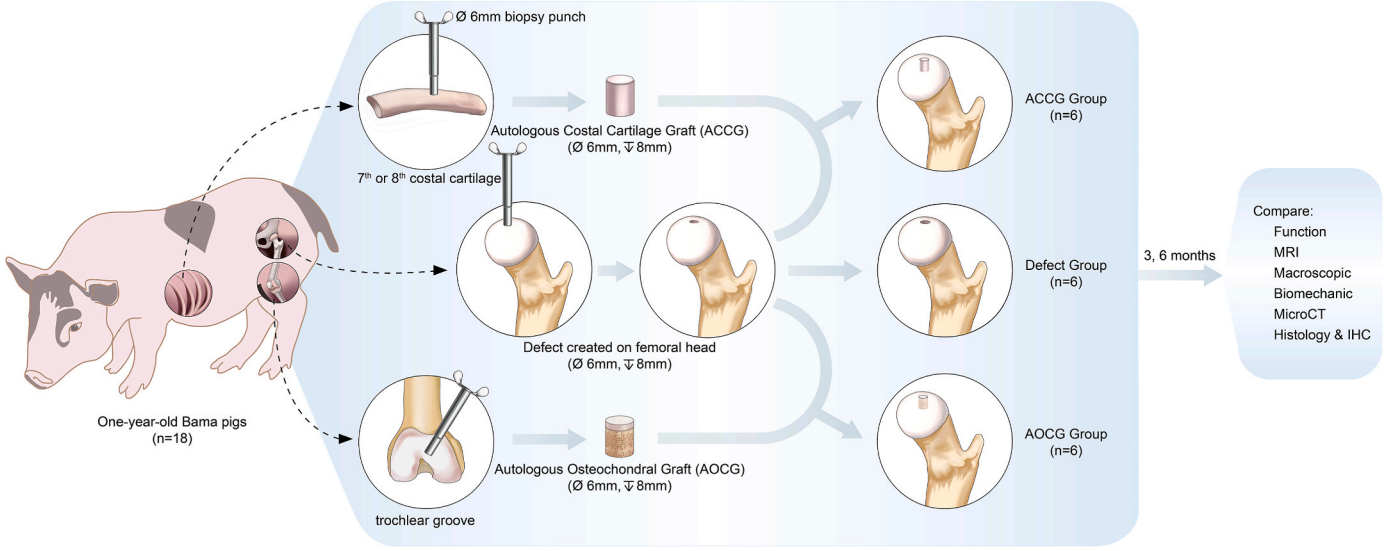

Fig. 1. Illustration of the experimental design
Fig. 1. Schematic representation of the surgical procedures in the defect and graft groups.
Osteochondral defect of femoral head was made through the lateral incision of the hip joint. AOCG was collected from the ipsilateral trochlear groove using a 6-mm diameter biopsy punch through a medial knee incision. ACCG was harvested from the right 7th or 8th costal cartilage. AOCG or ACCG was inserted into the defect area, ensuring no plug protrusion or sedimentation.

diameter biopsy punch with perichondrium carefully removed. The depth limitation design of the biopsy punch ensured that the harvested sample was consistent in diameter and depth. During the harvest procedure, care must be taken to avoid pneumothorax.

Defect creation: To create osteochondral defect of femoral head, an 8 cm long incision was made over the lateral side of the hip joint. After capsulotomy, the femur was abducted and externally rotated to expose the lateral weight-bearing zone of the femoral head. A biopsy punch was used to create an osteochondral defect (6 mm in diameter, 8 mm in depth). No plug protrusion or sedimentation was ensured after AOCG or ACCG was inserted into the defect area.

Wound was closed layer-by-layer with bioabsorbable sutures. After surgery, the animals were returned to the enclosures and monitored until full recovery. They were allowed to move freely without restrictions.

Postoperative hip function evaluation was performed at 3 and 6 months. Then, the Bama pigs were euthanized by hemorrhagic shock under pentobarbitone anesthesia. The entire hip joint including the acetabulum and femoral head was harvested for analysis.

2.3. Motor function assessment

Hip function was recorded by single-lens reflex camera (ILCE-7RM3, SONY) and was assessed using the porcine thoracic injury behavior scoring (PTIBS) system for locomotor behavior at 3 and 6 months after surgery [32]. The locomotor function of the Bama pigs was observed and assessed by trained researchers following previously described methods (Supplementary Table 2).

2.4. MRI

MRI examination was performed by 3-Tesla MR scanner (MAGNETOM, Prisma, Siemens Healthineers, Erlangen, Germany) on intact hip joints collected. Images were collected in the sagittal plane of the femoral head including following sequences: Proton Density Weighted Image (PDWI), T1WI and T2WI [33]. Modified magnetic resonance observation of cartilage repair tissue (MOCART) scoring system was used to evaluate the morphological status of the grafting plug and surrounding cartilage [34,35]. In specific, total modified MOCART score ranges from 0 to 100 as a collection of seven variables that include degree of defect filling, cartilage interface integration, surface, structure and signal intensity of the graft, bony defect, and subchondral changes (Supplementary Table 4).

2.5. Macroscopic observation

The macroscopic appearance was assessed according to the International Cartilage Repair Society (ICRS) macroscopic scoring system. Items include the degree of the defect filling, integration to the border zone and the appearance of repaired surface (0–4 points for each item, 12 points in total) (Supplementary Table 6) [36].

2.6. Biomechanical assessment

The nanoindentation test was used to analyze the hardness and elastic modulus [37]. Indentation was performed using the Hysitron TI 950 TriboIndenter nanomechanical testing system (Bruker, Ettlingen, Germany) to assess the biomechanical properties between the ACCG, AOCG and Defect groups. Briefly, the specimens were trimmed to fit in the modular of the mechanical testing device and at least 9 indentations were made on each sample to assess hardness and elastic modulus under depth-controlled mode (200 nm) at a constant loading and unloading rate of 20 nm/s and a 10-s hold at the peak depth. The elastic modulus was calculated from the unloading segment of the load-penetration depth curve following the Oliver-Pharr method. During the test, samples were kept moist with saline solution.

2.7. Micro-CT (μCT)

The samples were scanned by micro-tomograph 1076 scanner (Skyscan, Kontich, Belgium) for μCT analysis. The data were acquired at a resolution of 35 mm and reconstructed using a modified Feldkamp algorithm provided by Skyscan. Visualization and analysis were carried out with MIMICS (Materialize, Leuven, Belgium) and Ctan (Bruker, Ettlingen, Germany). The region of interest (ROI) was contoured in a cylinder with a diameter of 6 mm centered on the graft. Percent bone volume (BV/TV), trabecular number (Tb. N), trabecular separation (Tb. Sp), and trabecular thickness (Tb. Th) at different postoperative time points of AOCG and ACCG were analyzed.

2.8. Histology and immunohistochemistry (IHC)

The specimens were fixed in 4 % paraformaldehyde (PFA). After decalcification, ethanol dehydration, and paraffin embedding, serial sections (5-μm-thick) were stained with hematoxylin–eosin (H.E.), Masson's trichrome staining and ALP staining [38]. Immunohistochemistry (IHC) was conducted using anti-Collagen type I (Col1a1, monoclonal; dilution factor 1:500; Abcam), anti-Collagen type II (Col2a1, monoclonal, dilution factor 1:500; Abcam). Horseradish peroxidase-conjugated goat anti-rabbit IgG (1:2500; BA1055; Boster, Wuhan, China) was used as the secondary antibody [35]. Modified Mankin score was used to evaluate the severity of osteoarthritis of the femoral head [39] (Supplementary Table 7). For Goldner's trichrome staining, the specimens were prepared at 7-μm-thick for hard tissue sections.

2.9. Statistical analysis

Data were analyzed and presented using GraphPad Prism version 9.0. Descriptive statistics were reported as means, standard deviations (SD), medians, and minimum and maximum values. The Shapiro-Wilk test was used to assess the normality of the test score distributions. If the data followed a normal distribution, parametric statistics were applied. The significance of the differences between the tested and control samples (or different groups) was calculated using one-way ANOVA. The Šidák post hoc test was used to identify differences between the tested groups. P-values less than 0.05 were considered statistically significant.

3. Results

3.1. ACCG and AOCG show equivalent therapeutic effect in treating femoral head osteochondral defect

All the experimental animals in Defect, ACCG and AOCG groups recovered full range of motion within one week after surgery. The Porcine Thoracic Injury Behavior Scale (PTIBS) was used to assess the hip function in Bama pigs at postoperative 3 and 6 months. Functional assessment showed no significant difference in the activity between groups at postoperative 3 months (Defect: 10.00 ± 0.00, AOCG: 10.00 ± 0.00, ACCG: 10.00 ± 0.00) (Supplementary Table 3). However, the hip functions of Defect group declined significantly at postoperative 6 months (Defect: 8.67 ± 0.58, AOCG: 10.00 ± 0.00, ACCG: 10.00 ± 0.00; $p_{\text{DefectvsACCG}} = 0.006$; $p_{\text{DefectvsAOCG}} = 0.006$) (Supplementary Table 3). There was no sign of complications such as physical restriction, inflammation or swelling in all groups till euthanasia (Supplementary Table 8). Therefore, ACCG is effective in treating the osteochondral defect in the femoral head of Bama pig model and has yielded comparable therapeutic effect as AOCG provides.

3.2. Macroscopic appearance reveals equivalent reconstruction of femoral head osteochondral defect using AOCG and ACCG

During the sample collection, the Defect group exhibited irregular articular surface, localized growth of synovium and fibrous tissues, and degeneration of cartilage (Fig. 2b–c). All grafts in the ACCG group remained in place without separation, protrusion, or deposition (Fig. 2h and i). The cartilage surface of the AOCG (Fig. 2e and f) and ACCG exhibited a smooth and uniform texture, similar to that of the recipient joint surface. The ACCG (3 months: 10.67 ± 0.58, 6 months: 11.33 ± 0.58) and AOCG (3 months: 10.67 ± 0.58, 6 months:11.67 ± 0.58) groups showed significantly higher ICRS scores when compared to the Defect group (3 months: 6.67 ± 0.58, 6 months: 6.33 ± 0.58) at both 3 months ($p_{DefectvsACCG} < 0.001$; $p_{DefectvsAOCG} < 0.001$) and 6 months ($p_{DefectvsACCG} < 0.001$; $p_{DefectvsAOCG} < 0.001$). No significant difference was observed between the AOCG and ACCG groups at either time point (Fig. 2j).

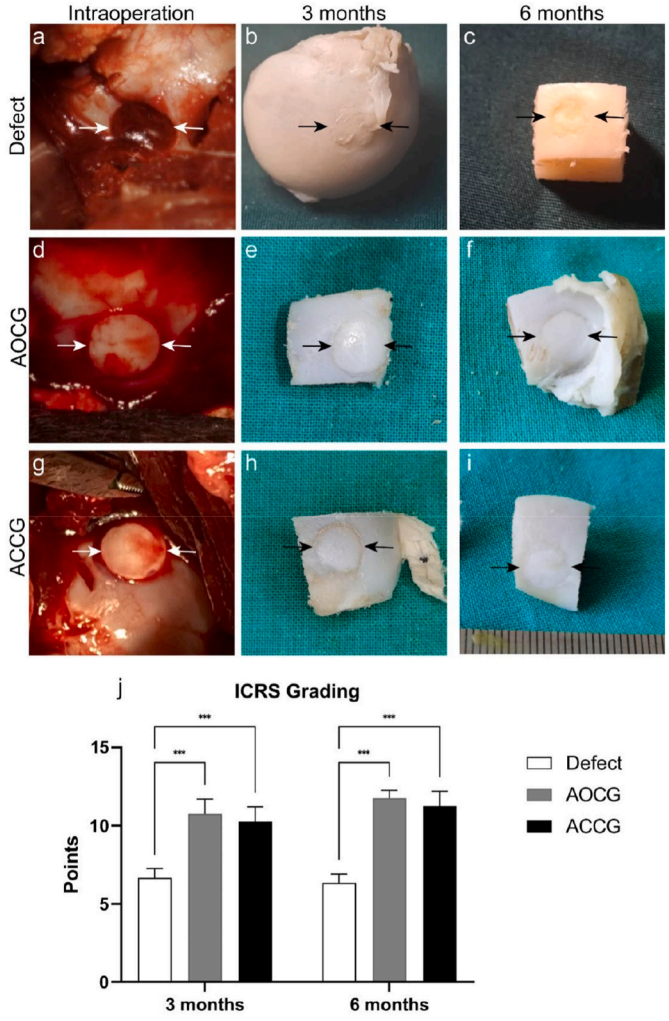

Fig. 2. Macroscopic observation and ICRS grading at different postoperative time points

Fig. 2. Macroscopic observation and ICRS grading. Intraoperative photographs of a Bama pig's femoral head articular surfaces from the defect, AOCG, and ACCG groups (a, d, g). Macroscopic observations at various postoperative time points (b, c, e, f, h, i). Arrows indicate the areas of defects or grafts. ICRS grading of the femoral head articular surfaces at different time points showed no statistical difference between the AOCG and ACCG groups, both differing significantly from the defect group (j). *p-value < 0.05, **p -value < 0.01, ***: p -value < 0.001.

3.3. ACCG repairs osteochondral defects and prevents hip joint degeneration

The modified MOCART score was employed to evaluate the repair status of the grafts (Supplementary Table 5). At 3 months, The AOCG group (90.00 ± 5.00) was significantly higher than that of the defective group (60.00 ± 5.00, $p < 0.001$) and the ACCG group (76.67 ± 2.89, $p = 0.01$). The ACCG group also had a significantly higher score compared to the Defect group ($p = 0.003$). By 6 months, the difference between the ACCG (81.67 ± 2.89) and AOCG (91.67 ± 5.77) groups had disappeared, with both groups demonstrating higher scores than the Defect group (56.67 ± 5.77, $p_{DefectvsACCG} < 0.001$; $p_{DefectvsAOCG} < 0.001$) and maintaining a statistically significant difference (Fig. 3g). In T2 sequence, we observed homogeneously lower signal intensity in ACCG at postoperative 6 months when compared with earlier time points, suggesting that the hyaline costal cartilage had been gradually replaced by bony tissue (Fig. 3e and f).

3.4. ACCG maintains the biomechanical properties of articular cartilage after implantation

To further evaluate the mechanical property of the implant, we performed nano indentation test. At 3 months, both AOCG (4.67 ± 0.88 MPa) and ACCG (3.13 ± 1.25 MPa) exhibited significantly lower elastic modulus when compared to the Defect group (23.97 ± 6.76 MPa, $p_{DefectvsACCG} = 0.001$; $p_{DefectvsAOCG} < 0.001$), while no significant difference was observed between AOCG and ACCG group ($p = 0.960$). The elastic module of ACCG remained stable at 6 months in comparison with 3 months ($p = 0.514$), with both AOCG (4.12 ± 1.86 MPa) and ACCG (4.03 ± 1.80 MPa) remained lower than Defect group (17.61 ± 6.42, $p_{DefectvsACCG} = 0.010$; $p_{DefectvsAOCG} = 0.020$), indicating that ACCG could maintain biomechanical property of hyaline cartilage after transplantation (Supplementary Fig. 1).

3.5. ACCG transplantation undergoes ossification in the subchondral region

To evaluate the trabecular status of two different grafts at different time points, μCT scan and quantitative analysis were performed (Fig. 4 & Supplementary Table 9). The mean percent bone volume (BV/TV) and trabecular number (Tb. N) of ACCG group were lower than AOCG group at 3 months (BV/TV (%): Defect:12.53 ± 8.24, AOCG: 52.42 ± 14.65%, ACCG: 12.81 ± 2.35, $p_{DefectvsACCG} = 0.004$; $p_{AOCGvsACCG} < 0.001$; Tb. N ($1/10^{-3}$μm): Defect: 0.69 ± 0.40, AOCG: 2.96 ± 0.50, ACCG: 0.58 ± 0.14, $p_{DefectvsAOCG} < 0.001$; $p_{AOCGvsACCG} < 0.001$), yet gradually increased until no significant difference of BV/TV was shown at 6 months in comparison with AOCG (BV/TV (%): Defect: 38.17 ± 1.45, AOCG: 48.01 ± 17.75, ACCG: 33.67 ± 12.54, $p_{DefectvsAOCG} = 0.911$; $p_{AOCGvsACCG} = 0.433$; Tb. N ($1/10^{-3}$μm): Defect: 1.92 ± 0.11, AOCG: 3.55 ± 0.14, ACCG: 1.98 ± 0.66, $p_{DefectvsAOCG} = 0.003$; $p_{AOCGvsACCG} < 0.001$), indicating the ossification of ACCG in the subchondral region. At 6 months, though the Defect group exhibited an increase of BV/TV and Tb. N, the trabecular separation (Tb. Sp) remained significantly higher than AOCG and ACCG (3 months: Defect: 1678.89 ± 618.59 μm, AOCG: 266.09 ± 64.51 μm, ACCG: 1200.86 ± 306.05 μm, $p_{DefectvsAOCG} < 0.001$; $p_{AOCGvsACCG} = 0.002$; 6 months: Defect: 1178.12 ± 118.34 μm, AOCG: 179.55 ± 24.16 μm, ACCG: 553.97 ± 334.85 μm, $p_{DefectvsAOCG} < 0.001$; $p_{DefectvsACCG} = 0.031$). No difference of Tb. Sp was observed between ACCG and AOCG at 6 months ($p = 0.248$). Collectively, these results indicate that ACCG implant underwent ossification in the subchondral region, which favor the reconstruction of subchondral bone (Fig. 4m–p).

3.6. ACCG remains hyaline articular surface while subchondral ossification occurs

The sections of femoral head articular surface of three groups

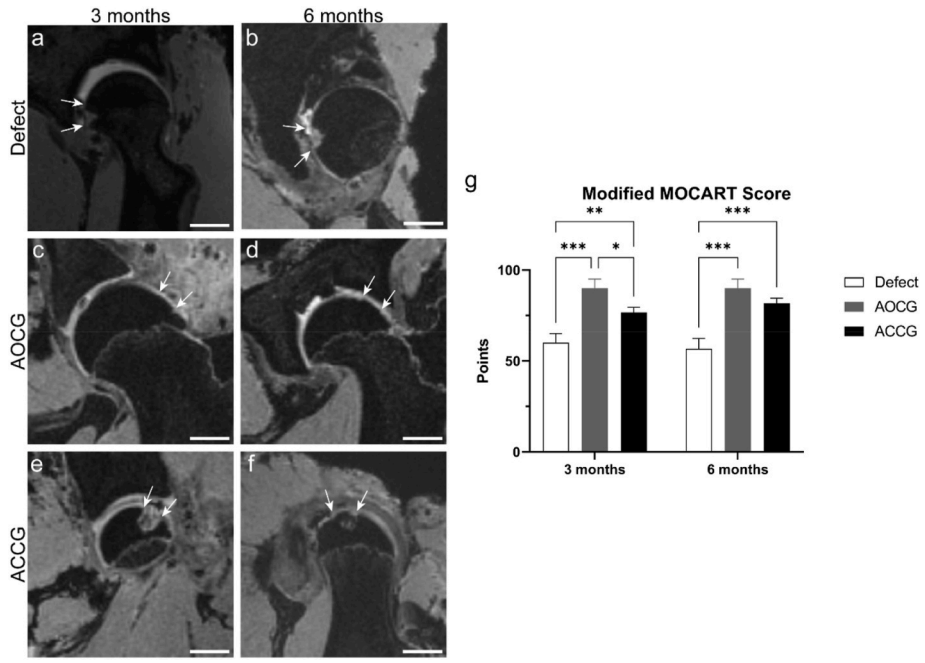

Fig. 3. MRI assessment at different postoperative time points

Fig. 3. MRI examination at different postoperative time points. T2 sequences of femoral head without grafting: Defect (a, b), transplanted with AOCG (c, d) or ACCG (e, f) at different postoperative time points. White arrows indicate the margin of the defect or grafts. (g) Modified MOCART score at different postoperative time points. Scale bar = 1 cm. *p-value < 0.05, **p -value < 0.01, ***p -value≤0.001.

underwent histological assessment using H.E., Masson, and Goldner staining. In the Defect group, the defect was filled with fibrocartilage and fibrous tissues on the joint surface while abnormal cartilage structure with degenerative cartilage was formed adjacent to the defect site (Fig. 5A-D, M-P). The autologous grafts of both ACCG and AOCG survived and could be observed *in situ* at all time points (Fig. 5E-L, Q-X). Interestingly, the subchondral portion of the ACCG gradually ossified while the cartilage surface of the ACCG group remained cartilaginous and smooth (Fig. 5Q–X). Mankin scores showed no difference between AOCG (3 months: 2.67 ± 1.16; 6 months: 2.33 ± 1.53) and ACCG (3 months: 3.67 ± 0.58; 6 months: 4.33 ± 0.58) groups at either time points, while the Defect group (3 months: 6.67 ± 0.58; 6 months: 8.00 ± 1.00) had significantly higher Mankin score when compared to AOCG group and ACCG group at both time points (3 months: $p_{\text{DefectvsAOCG}} < 0.001$; $p_{\text{DefectvsACCG}} = 0.008$; 6 months: $p_{\text{DefectvsAOCG}} < 0.001$; $p_{\text{DefectvsACCG}} = 0.002$) (Supplementary Fig. 2). At 3 and 6 months, despite the good integration of the subchondral bone, the AOCG group still showed fissures at the junction of the cartilaginous surface between the grafts and recipient cartilage (Fig. 5 G, H, S, T). Conversely, at 3 months, the ACCG group demonstrated superior integration with the recipient articular cartilage and showed rich extracellular matrix composed of type II collagen in both recipient articular cartilage and ACCG (Fig. 5K, W, k, w), indicating that the repair tissue possessed characteristics similar to the extracellular matrix of recipient hyaline cartilage at the surface (Fig. 5 q-t, u-x). On the other hand, type I collagen staining of the cartilage surface of ACCG as well as the tissue junctions was negative, suggesting that the surface of ACCG did not undergo ossification (Fig. 5i-l).

Further observation of the ACCG group revealed multiple porous ossification centers within the grafts at 3 months postoperatively (Fig. 6 A-R). After 6 months, the subchondral bone portion of ACCG showed significant increase in the extent of ossification (Fig. 6a–r). In ACCG, these ossification centers co-localized with the type I collagen expression observed at as early as 3 months after operation (Fig. 6 D), while the type II collagen staining disappeared from the type I collagen-positive areas (Fig. 6 E). In collection with the previous uCT results, IHC findings favor an endochondral ossification-like process (Fig. 6).

4. Discussion

Osteochondral defects, prevalent in athletes and the elderly, are a major risk factor for the development of osteoarthritis, necessitating effective treatment strategies. Abnormal biomechanical loading at the edges of these defects can promote osteoarthritis in the adjacent cartilage [40]. Currently, various experiments suggest that the treatment for repairing deep osteochondral defects in cartilage is limited [41]. Additionally, artificial “off-the-shelf” implants like scaffolds have demonstrated poor clinical outcomes with revision rates as high as 70 % [42,43]. While AOCG is a promising treatment method for osteochondral defect, it has limitations such as scarcity of donor materials and morbidity at the donor sites [44]. Moreover, the joint surface reconstructed by AOCG combines hyaline and fibrous cartilage as gaps between the multiple AOCG plugs are filled with fibrous tissue, leading to poor biomechanical properties and durability [45]. Therefore, it is prompt to find a reliable and abundant autologous source for osteochondral defect repair while minimizing donor site morbidity.

Costal cartilage not only has a composition similar to the articular cartilage but also has sufficient cell yield and fast ex vivo proliferation rates [46–48]. Costal cartilage has been utilized in various surgical procedures, including rhinoplasty and auricular reconstruction [49,50]. Moreover, the donor-site of costal cartilage can provide a sufficient source of hyaline cartilage and exhibits low morbidity [51]. Previously in a rabbit model, ACCG transplantation has repaired the knee osteochondral defect through biological integration with the subchondral bone. ACCG formed solid osteochondral interface structure and maintained hyaline cartilage morphology [28,29]. But its therapeutic efficacy in large animal model has not been tested. Therefore, this study is designed to investigate the efficacy of using ACCG to repair osteochondral defect in deep weight-bearing hip joint using femoral head osteochondral defect model in Bama pigs.

In the treatment groups, we implanted either AOCG or ACCG into the osteochondral defect created in the weight-bearing area of a femoral

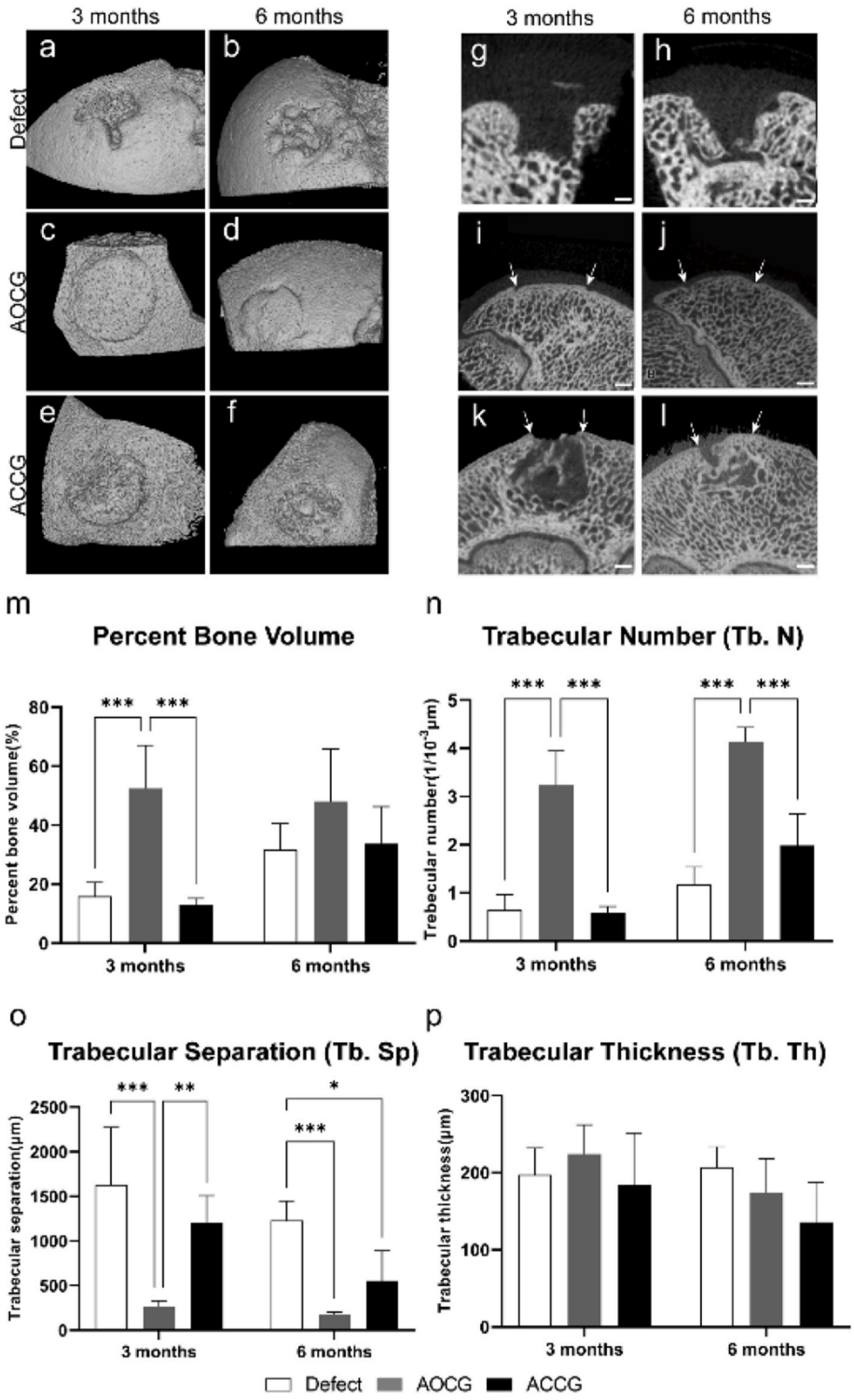

Fig. 4. μCT assessment at different postoperative time points

Fig. 4 μCT assessment at different postoperative time points. (a–f) Three-dimensional reconstruction of subchondral bone and (g–i) cross-sections of μCT scan of defect, AOCG and ACCG at different postoperative time points. White arrows indicate the margin of defect or grafts. Scale bar = mm. (m) Percent bone volume (BV/TV), (n) trabecular number (Tb. N), (o) trabecular separation (Tb. Sp) and (p) trabecular thickness (Tb. Th) at different postoperative time points. Scale bar = 1 mm. *p-value < 0.05, **p -value < 0.01, ***p -value≤0.001.

head. The results of the PTIBS have provided an important insight into the functional recovery of the subjects following treatment. At 3 months, all groups had achieved perfect scores, indicating comparable functional recovery in the early phase. However, by 6 months, the functional outcome of the Defect group declined slightly and was significantly lower than that of the ACCG and AOCG groups. These results suggested that although the Defect group managed to compensate the lower limb activities initially, the Defect group gradually manifested with symptomatic activity limitation over time, whereas the treated groups continued maintaining better functional performance. This is consistent

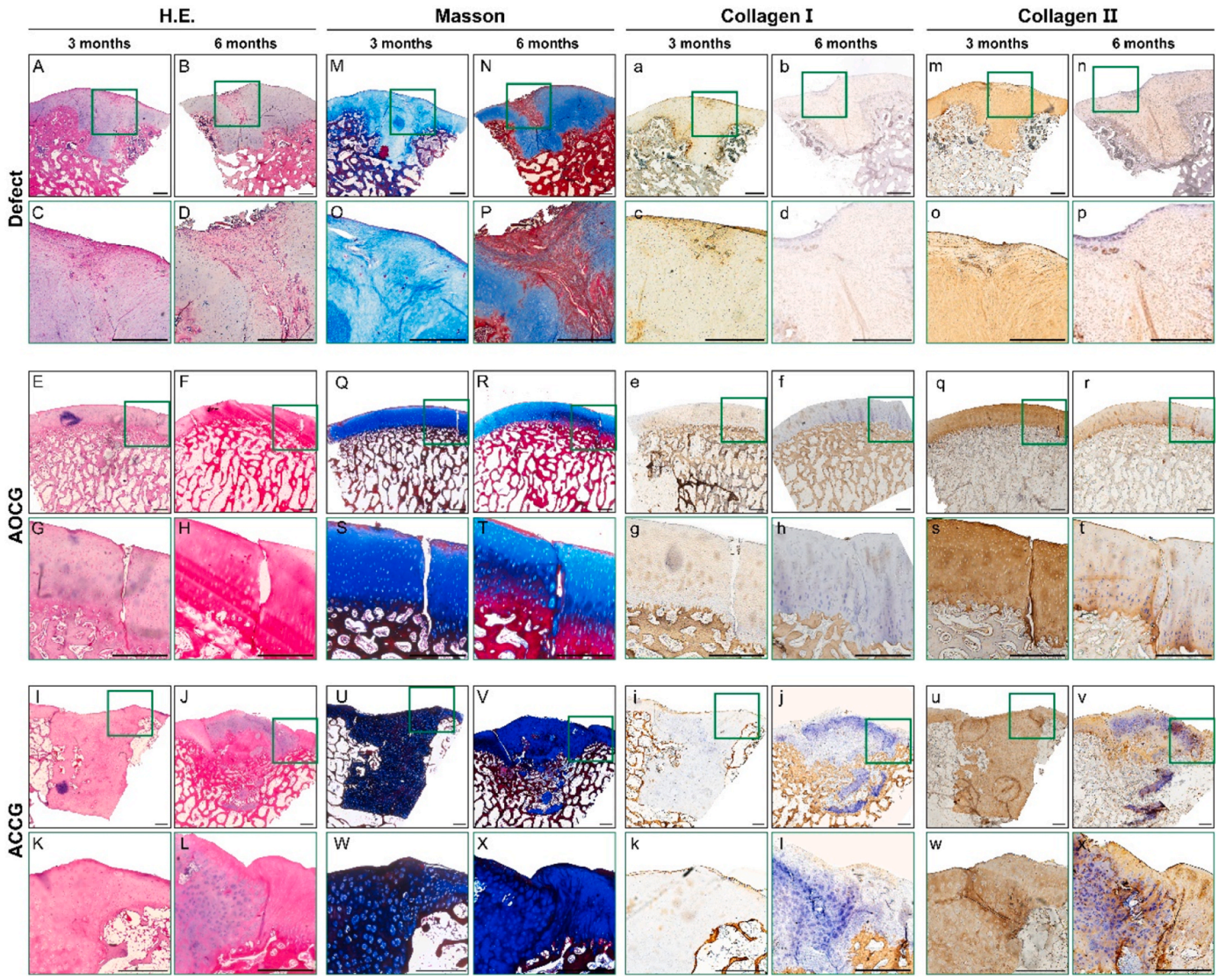

Fig. 5. Histology assessment at different postoperative time points

Fig. 5. Histology assessment of Defect, AOCG and ACCG at different postoperative time points with overall view and magnified view. (A–L) H.E. staining, (M–X) Masson staining, (a–l) Collagen I staining and (m–x) Collagen II staining of femoral head articular surface at different postoperative time points. The green box are magnified views of the zoomed-in area. Scale bar = 1 mm. (For interpretation of the references to colour in this figure legend, the reader is referred to the Web version of this article.)

with our imaging and histologic findings.

Both implants remained stable in situ and maintained smooth surfaces without exposed bone tissue or synovitis symptoms. The ICRS scores indicated that there was no macroscopic difference between the AOCG and ACCG at all time points. The MRI showed no significant signal changes in AOCG or ACCG surface. H.E., Masson, ALP and IHC staining demonstrated that the superficial layer of ACCG at the joint surface maintained the morphology of hyaline cartilage. Ma et al. reported that the synovial membrane can maintain the costal cartilage phenotype and thus prevents hypertrophic differentiation during cartilage repair [52]. Liu et al. reported that the avascular, absence of neural innervation, hypoxic microenvironment helps maintain the current form of hyaline cartilage [53], which explains the absence of significant degeneration or ossification on the surface of ACCG. More importantly, small fissures at the graft–cartilage interface with recipient tissue in AOCG were observed, indicating poor regenerative capacity. On the other hand, costal cartilage formed integrated interface between the surrounding articular cartilage and ACCG-repaired osteochondral defect, indicating its regenerative potential.

In addition to the superficial cartilage layer, the remodeling of subchondral bone is equally crucial. The AOCG group, regarded as the gold standard for osteochondral defect repair, exhibited a higher bony signal on the modified MOCART score when compared to ACCG group at 3 months. By 6 months, the bony signal of ACCG had increased which is indicative of the remodeling of subchondral portion in ACCG. μCT analysis of the subchondral structure revealed that AOCG constantly had higher trabecular number and lower trabecular separation values at all time points when compared to ACCG. Interestingly, from postoperative 3–6 months, there was a significant increase in both trabecular number and percent bone volume in the ACCG group. By 6 months, the percent bone volume in ACCG was comparable to that of AOCG, further demonstrating that the embedded costal cartilage grafts had been undergoing a remodeling process to form trabecular bone. Importantly, the remodeled trabecular bone in the ACCG matched the thickness of the recipient's trabecular bone, indicating that the ACCG's ossified layer truly became mechanically functional subchondral bone [54,55]. At 6 months, the functional, histological and radiographic outcomes for both ACCG and AOCG were similar and superior to the Defect group, further

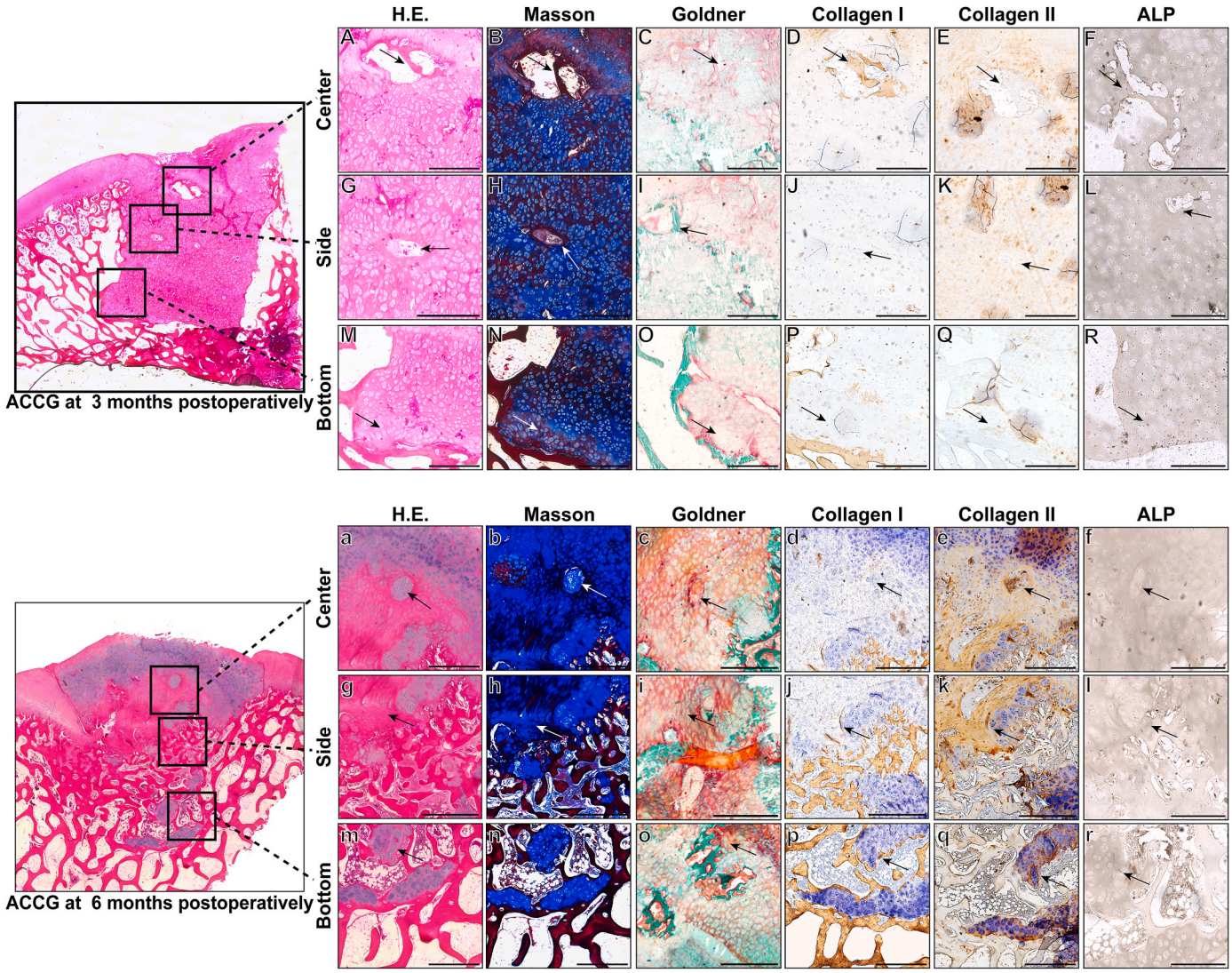

Fig. 6. Histology evaluation of ACCG over time
Fig. 6. Magnified views of different areas on ACCG at different postoperative time points. (A-F, a-f) Center area of the costal cartilage graft. (G-L. g-l). Side area of the costal cartilage graft. (M-R, m-r) Bottom area of the costal cartilage graft. The arrows indicate the locations where endochondral ossification occurs. Scale bar = 1 mm.

suggesting that ACCG is a feasible, effective and safe method for repairing femoral head osteochondral defect without sacrificing the donor joint.

Histological assessment revealed that both AOCG and ACCG exhibited excellent integration at the graft–bone interface, ensuring the anatomical stability of the grafts. Most interestingly, by 3 months postoperatively, ACCG sections had shown multiple scattered ossification centers beneath the subchondral bone, which was also confirmed by μCT and modified MOCART. These multicentric ossification centers were located not only around the bone-graft interface but also within the center of the costal cartilage grafts, where clusters of cartilage cells and large cartilage lacunae were observed. By 6 months, these subchondral ossification centers have gradually merged and were replaced by trabecular bone, which integrated stably with the recipient tissue [38]. Pang et al. demonstrated previously that when the costal cartilage was transplanted into mouse knee joints, blood vessels could invade the grafts at the bone interface, thereby initiating the endochondral ossification [50]. Therefore, the observed endochondral ossification-like process might explain the remodeling of ACCG at subchondral layer after transplantation.

By elucidating the signaling pathways involved in the endochondral ossification observed in ACCG and through long-term study to explore the prognosis of ACCG-repaired femoral head. Once the effectiveness of this proposed method is verified, ACCG can be potentially translated into practical therapy to treat large-scale osteochondral lesions in the weight-bearing joint in human.

Future investigation is needed to elucidate the possible signaling pathways involved in the endochondral ossification observed in ACCG. Long-term studies will be performed to explore the prognosis between AOCG and ACCG to validate their clinical effectiveness. Additionally, we used Bama pigs as the large animal model in this study. Due to the differences in the weight-bearing mechanics between bipeds (human) and quadrupeds (Bama pigs), osteochondral repair process may vary.

5. Conclusion

In summary, ACCG shows promise as a treatment for femoral head osteochondral defects. During the repair process, we have observed an intriguing endochondral ossification-like remodeling in ACCG, where it transforms into an articular osteochondral unit after being transplanted into the joint environment. Furthermore, costal cartilage is an affluent and readily available hyaline cartilage source with minimal donor-site

morbidity. Lastly, it is worth noting that the short-term repair efficacy using ACCG was not inferior to that provided by AOCG in terms of treating femoral head osteochondral lesion in a swine model.

Ethical committee approval

Each author certifies that his or her institution has approved the animal protocol for this investigation, that all investigations were conducted in conformity with ethical principles of as outlined on title page (with all required information). No informed consent for participation was needed in the study.

Conflicts of interest

The authors declare that they have no conflicts of interest. This study was supported by the National Natural Science Foundation of China (Grant 81820108020, 82002340).

Acknowledgements

All persons who have made substantial contributions to the work reported in the manuscript (e.g., techni-cal help, writing and editing assistance, general support), but who do not meet the criteria for authorship, are named in the Acknowledgements and have given us their written permission to be named. If we have not included an Acknowledgements, then that indicates that we have not received substantial contributions from non-authors.

Appendix A. Supplementary data

Supplementary data to this article can be found online at https://doi.org/10.1016/j.jot.2024.10.007.

References

[1] Beck M, Kalhor M, Leunig M, Ganz RJ, Volume JSB. Hip morphology influences the pattern of damage to the acetabular cartilage: femoroacetabular impingement as a cause of early osteoarthritis of the hip 2005;87(7):1012–8.
[2] Hunter DJ, Bierma-Zeinstra S. Osteoarthritis. Lancet 2019;393(10182):1745–59 [eng].
[3] Sellards RA, Nho SJ, Cole BJ. Chondral injuries 2002;14(2):134–41.
[4] Hunziker EBJO. Articular cartilage repair: basic science and clinical progress. A review of the current status and prospects 2002;10(6):432–63. cartilage.
[5] Schinhan M, Gruber M, Vavken P, Dorotka R, Samouh L, Chiari C, et al. Critical-size defect induces unicompartmental osteoarthritis in a stable ovine knee 2012;30(2):214–20.
[6] Miller RE, Grodzinsky AJ, Barrett MF, Hung H-H, Frank EH, Werpy NM, et al. Effects of the combination of microfracture and self-assembling peptide filling on the repair of a clinically relevant trochlear defect in an equine model 2014;96(19):1601–9.
[7] Badekas T, Takvorian M, Njio Souras. Treatment principles for osteochondral lesions in foot and ankle, vol. 37; 2013. p. 1697–706.
[8] Christensen BB, Foldager CB, Olesen ML, Hede KC, Lind MJ. Implantation of autologous cartilage chips improves cartilage repair tissue quality in osteochondral defects: a study in Göttingen minipigs 2016;44(6):1597–604.
[9] El Bitar YF, Lindner D, Jackson TJ, Domb BGJJ, JotAAoOS. Joint-preserving surgical options for management of chondral injuries of the hip 2014;22(1):46–56.
[10] Hackney LA, Lee MH, Joseph GB, Vail TP, Link TM. Subchondral insufficiency fractures of the femoral head: associated imaging findings and predictors of clinical progression, vol. 26; 2016. p. 1929–41.
[11] Huang BJ, Hu JC, Athanasiou KAJB. Cell-based tissue engineering strategies used in the clinical repair of articular cartilage, vol. 98; 2016. p. 1–22.
[12] Muthu S, Korpershoek JV, Novais EJ, Tawy GF, Hollander AP, Martin I. Failure of cartilage regeneration: emerging hypotheses and related therapeutic strategies. Nat Rev Rheumatol 2023;19(7):403–16 [eng].
[13] Murawski CD, Kennedy JGJJ. Operative treatment of osteochondral lesions of the talus 2013;95(11):1045–54.
[14] Medvedeva EV, Grebenik EA, Gornostaeva SN, Telpuhov VI, Lychagin AV, Timashev PS, et al. Repair of damaged articular cartilage: current approaches and future directions 2018;19(8):2366.
[15] Harris JD, Brophy RH, Siston RA, DcjatjoA Flanigan, Surgery R. Treatment of chondral defects in the athlete's knee 2010;26(6):841–52.
[16] Hangody L, Füles PJJ. Autologous osteochondral mosaicplasty for the treatment of full-thickness defects of weight-bearing joints: ten years of experimental and clinical experience 2003;85(suppl_2):25–32.
[17] Kääb M, Ap Gwynn I, HjtjoA Nötzli. Collagen fibre arrangement in the tibial plateau articular cartilage of man and other mammalian species 1998;193(1):23–34.
[18] Khanna V, Tushinski D, Drexler M, Backstein D, Gross A, Safir O, et al. Cartilage restoration of the hip using fresh osteochondral allograft: resurfacing the potholes, vol. 96; 2014. p. 11–6. 11_Supple_A.
[19] Kosashvili Y, Raz G, Backstein D, Lulu OB, Gross AE, Safir OJIo. Fresh-stored osteochondral allografts for the treatment of femoral head defects: surgical technique and preliminary results, vol. 37; 2013. p. 1001–6.
[20] Looze CA, Capo J, Ryan MK, Begly JP, Chapman C, Swanson D, et al. Evaluation and management of osteochondral lesions of the talus 2017;8(1):19–30.
[21] Mei XY, Alshaygy IS, Safir OA, Gross AE, PrjtjoA Kuzyk. Fresh osteochondral allograft transplantation for treatment of large cartilage defects of the femoral head: a minimum two-year follow-up study of twenty-two patients 2018;33(7):2050–6.
[22] Hangody L, Vásárhelyi G, Hangody LR, Sükösd Z, Tibay G, Bartha L, et al. Autologous osteochondral grafting—technique and long-term results 2008;39(1):32–9.
[23] Feczkó P, Hangody L, Varga J, Bartha L, Diószegi Z, Bodó G, et al. Experimental results of donor site filling for autologous osteochondral mosaicplasty 2003;19(7):755–61.
[24] Sajjadian A, Rubinstein R, Naghshineh NJP, surgery r. Current status of grafts and implants in rhinoplasty: part I. Autologous grafts 2010;125(2):40e–9e.
[25] Zappaterra T, Obert L, Pauchot J, Lepage D, Rochet S, Gallinet D, et al. Post-traumatic reconstruction of digital joints by costal cartilage grafting: a preliminary prospective study 2010;29(5):294–300.
[26] Thomsen NO, Wikström S-O, Müller G, Dahlin LBJ. Costal osteochondral graft for total metacarpal head replacement due to extensive osteochondral lesion, vol. 19; 2014. p. 1036–9.
[27] Shimada K, Tanaka H, Matsumoto T, Miyake J, Higuchi H, Gamo K, et al. Cylindrical costal osteochondral autograft for reconstruction of large defects of the capitellum due to osteochondritis dissecans 2012;94(11):992–1002.
[28] Du D, Hsu P, Zhu Z, Zhang CJJoot. Current surgical options and innovation for repairing articular cartilage defects in the femoral head, vol. 21; 2020. p. 122–8.
[29] Gao Y, Gao J, Li H, Du D, Jin D, Zheng M, et al. Autologous costal chondral transplantation and costa-derived chondrocyte implantation: emerging surgical techniques, vol. 11; 2019, 1759720X19877131.
[30] Swindle MM, Smith AC, BjjjoIS Hepburn. Swine as models in experimental surgery 1988;1(1):65–79.
[31] Chu CR, Szczodry M, Bruno SJ. Animal models for cartilage regeneration and repair 2010;16(1):105–15.
[32] Lee JH, Jones CF, Okon EB, Anderson L, Tigchelaar S, Kooner P, et al. A novel porcine model of traumatic thoracic spinal cord injury. J Neurotrauma 2013;30(3):142–59 [eng].
[33] Marlovits S, Striessnig G, Resinger CT, Aldrian SM, Vecsei V, Imhof H, et al. Definition of pertinent parameters for the evaluation of articular cartilage repair tissue with high-resolution magnetic resonance imaging 2004;52(3):310–9.
[34] Bittersohl B, Miese FR, Hosalkar HS, Herten M, Antoch G, Krauspe R, et al. T2* mapping of hip joint cartilage in various histological grades of degeneration. Osteoarthritis Cartilage 2012;20(7):653–60 [eng].
[35] Schreiner MM, Raudner M, Marlovits S, Bohndorf K, Weber M, Zalaudek M, et al. The MOCART (magnetic resonance observation of cartilage repair tissue) 2.0 knee score and atlas. Cartilage 2021;13(1_suppl). 571S-87S. [eng].
[36] Widuchowski W, Widuchowski J, Trzaska TJTK. Articular cartilage defects: study of 25. 124 knee arthroscopies 2007;14(3):177–82.
[37] Zuo Q, Cui W, Liu F, Wang Q, Chen Z, Fan W. Utilizing tissue-engineered cartilage or BMNC-PLGA composites to fill empty spaces during autologous osteochondral mosaicplasty in porcine knees. (1932-7005 (Electronic)). [eng]..
[38] Nie W, Peng C, Zhou X, Chen L, Wang W, Zhang Y, et al. Three-dimensional porous scaffold by self-assembly of reduced graphene oxide and nano-hydroxyapatite composites for bone tissue engineering. Carbon 2017;116:325–37.
[39] Zhang J, Song GY, Chen XZ, Li Y, Li X, Zhou JL. Macroscopic and histological evaluations of meniscal allograft transplantation using gamma irradiated meniscus: a comparative in vivo animal study. Chin Med J (Engl) 2015;128(10):1370–5 [eng].
[40] Gotterbarm T, Breusch SJ, Vilei SB, Mainil-Varlet P, Richter W, Jung MJIo. No effect of subperiosteal growth factor application on periosteal neo-chondrogenesis in osteoperiosteal bone grafts for osteochondral defect repair, vol. 37; 2013. p. 1171–8.
[41] Maglio M, Brogini S, Pagani S, Giavaresi G, Tschon MJBRI. Current trends in the evaluation of osteochondral lesion treatments: histology, histomorphometry, and biomechanics in preclinical models. 2019;2019.
[42] Joshi N, Reverte-Vinaixa M, Díaz-Ferreiro EW, Domínguez-Oronoz RJTAjosm. Synthetic resorbable scaffolds for the treatment of isolated patellofemoral cartilage defects in young patients: magnetic resonance imaging and clinical evaluation 2012;40(6):1289–95.
[43] Dhollander AA, Liekens K, Almqvist KF, Verdonk R, Lambrecht S, Elewaut D, et al. A pilot study of the use of an osteochondral scaffold plug for cartilage repair in the knee and how to deal with early clinical failures 2012;28(2):225–33.
[44] Filardo G, Kon E, Perdisa F, Balboni F, Marcacci M. Autologous osteochondral transplantation for the treatment of knee lesions: results and limitations at two years' follow-up. Int Orthop 2014;38(9):1905–12 [eng].
[45] Zuo Q, Cui W, Liu F, Wang Q, Chen Z, Fan WJ, et al. Utilizing tissue-engineered cartilage or BMNC-PLGA composites to fill empty spaces during autologous osteochondral mosaicplasty in porcine knees 2016;10(11):916–26.

[46] Ishizeki K, Shinagawa T, Nawa T. Origin-associated features of chondrocytes in mouse Meckel's cartilage and costal cartilage: an in vitro study. Ann Anat 2003; 185(5):403–10 [eng].
[47] Huwe LW, Brown WE, Hu JC, Athanasiou KA. Characterization of costal cartilage and its suitability as a cell source for articular cartilage tissue engineering. J Tissue Eng Regen Med 2018;12(5):1163–76 [eng].
[48] Lee J, Lee E, Kim HY, Son Y. Comparison of articular cartilage with costal cartilage in initial cell yield, degree of dedifferentiation during expansion and redifferentiation capacity. Biotechnol Appl Biochem 2007;48(Pt 3):149–58 [eng].
[49] Matsumoto K, Maeda M, Fujikawa M. Staged, laminated, costal cartilage framework for ear reconstruction. Clin Plast Surg 1990;17(2):273–85 [eng].
[50] Fedok FG. Costal cartilage grafts in rhinoplasty. Clin Plast Surg 2016;43(1):201–12 [eng].
[51] Jenny HE, Siegel N, Yang R, Redett RJ. Safety of irradiated homologous costal cartilage graft in cleft rhinoplasty. Plast Reconstr Surg 2021;147(1):76e–81e [eng].
[52] Ma Y, Zheng K, Pang Y, Xiang F, Gao J, Zhang C, et al. Anti-hypertrophic effect of synovium-derived stromal cells on costal chondrocytes promotes cartilage repairs. J Orthop Translat 2022;32:59–68 [eng].
[53] Liu Y, Shah KM, Luo J. Strategies for articular cartilage repair and regeneration. Front Bioeng Biotechnol 2021;9:770655 [eng].
[54] Huang Y, Fan H, Gong X, Yang L, Wang F. Scaffold with natural calcified cartilage zone for osteochondral defect repair in minipigs. Am J Sports Med 2021;49(7): 1883–91 [eng].
[55] Keaveny TM, Morgan EF, Niebur GL, Yeh OC. Biomechanics of trabecular bone. Annu Rev Biomed Eng 2001;3:307–33 [eng].